

Multi-wavelength IR Method for Monitoring Air Pollution in Cities

Sergey Fanchenko^{a,b,*}, Alexander Baranov^a, Alexey Savkin^a
^a Moscow Aviation Institute (National Research University)
Moscow, Russia
^bNRC “Kurchatov Institute”
Moscow, Russia
fanchenko.sergey@kia.ru

Andrey Somov^c
College of Engineering, Mathematics and Physical Sciences, University of Exeter, UK

Lucia Calliari^d
FBK, Povo (Trento), Italy

Abstract—In this work we address the problem of air pollution in modern cities. We propose a method for detection and analysis of evaporation (H_2O), carbon dioxide (CO_2), carbon monoxide (CO) and methane (CH_4) which are the typical components of exhaust gases produced by the gasoline vehicles. The method is based on infrared multi-wavelengths absorption in the range of 1.3 – 2.3 μm and can be implemented by using multi waves array of light emitting diodes (LEDs). The proposed approach allows several absorption spectra to be covered by one LED absorption line, thus the number of used LEDs should be not less than the number of considered absorption lines. The simulation was done for a 6-element multi-wavelengths LED array. We demonstrate that the method is highly relevant for the application to open-path detectors where the radiation source and the receiver are located at a distance of tens of meters from each other.

Keywords—multicomponent toxic gas analysis; multi-wavelength near infrared spectroscopy, LED arrays, simulation

I. INTRODUCTION

Air pollution monitoring is an important task in many cities worldwide. This problem is reinforced by recent forecasts of the United Nations Population Fund: approximately 60 percent of the world population will move to an urban environment and 27 megacities with more than 10 million people will appear by 2030 [1]. Air pollution may have a severe impact on human health, e.g. cause cardiovascular and asthma diseases, and on environment [2]. To guarantee viable living conditions and sustainable city development urgent solutions are needed.

At the same time, the tremendous development of information and communication technologies have already helped to deploy a number of monitoring solutions in cities [3] and city infrastructure, e.g. road tunnels [4]. For example, mobile sensing [5], wireless sensor network (WSN) [6] and vehicular network [7] paradigms ensure real-time air quality sensing and can be integrated in existing city monitoring facilities using the power of Internet [8].

Widely used sensing technologies are built around electrochemical [9], semiconductor [10] and optical sensors [11]. The principle of operation of most optical sensors is based

on infrared (IR) spectroscopy.

IR spectroscopy in the near-IR range is a helpful technology to realize both local and remote sensing using non dispersive IR (NDIR) sensors.

For example, it can ensure gas detection along the perimeter of industrial premises or along pipelines [12, 13]. The NDIR method is also widely used for exhaust gas analysis. The main components of NDIR sensors are an IR lamp (also referred to as IR micro-heater), a measuring chamber, wavelength filters and an IR detector. The gas to be analyzed is pumped or diffused into the measuring chamber, and the concentration of target gases is measured by absorption of a specific wavelength for selected gas molecules. Typical strong absorption bands are in the 3.3-5 μm range (HITRAN database [14]). These sensors significantly outstrip electrochemical and semiconductor sensors in sensitivity, selectivity and response time. Moreover, they resist to harsh environment, they cannot be poisoned by high concentrations of the gases to be monitored and they are able to operate in anoxic environment. However, optical sensors are more power hungry with respect to the electrochemical and semiconductor ones. This fact might prevent their application in autonomous battery powered monitoring systems, e.g. WSN. High power demands may significantly reduce further adaptation of optical sensors to the needs of state-of-the-art systems dealing with gas analysis: creation of autonomous, miniaturized gas detectors and unattended monitoring devices with a wireless interface.

Recently developed Light Emitting Diodes (LEDs) operating in the 1.3 – 2.3 μm wavelength range open up new horizons for multicomponent exhaust gas analysis, especially for the detection of CO , CO_2 , CH_4 , H_2O exhaust gas components.

In this work, we present NDIR multicomponent gas analysis method based on infrared multi-wavelength LEDs in combination with a Photodiode (PD). The LEDs wavelengths are selected within the 1.3 – 2.3 μm wavelength range in such a way that cross sensitivity to different gases is excluded without the need of additional optical filter.

To date, there are no optical methods in the 1.3-2.3 μm wavelength range for detecting multicomponent gas mixtures

This work was supported by the grant No. RFMEFI57714X0022 from the Ministry of Education and Science of Russian Federation.

in the atmosphere. The advantage of using a wavelength in the 1.3-2.3 μm range is in the band gap of emitting semiconductor structures. The energy band gap of a LED material is 0.54 eV at a wavelength of 2.3 μm . As a result, the LED can be used without forced cooling, its temperature stabilization mechanism being enough for proper operation. IR lamps (or heaters) are mostly used in the 3.3-5 μm range. However, using semiconductor LEDs at wavelengths higher than 3.3 μm is rather pointless, due to the narrow energy band gap around 0.38 eV. In fact, even at normal temperature intrinsic conductance takes place, causing the semiconductor conductance to strongly depend on the temperature. In this case radiation recombination in the semiconductor drops drastically. The use of a multi-wavelength LED matrix improves the NDIR gas analysis as compared to one wavelength optical sensors [11].

The paper is organized as follows: in Section II we introduce the reader to the LED arrays used in this work and present the multi wavelength analysis method. Results obtained in this work are given in Section III. Finally, we summarize our work and provide concluding remarks in Section IV.

II. MULTIWAVELENGTH ANALYSIS METHOD

A. LED arrays for optical gas sensing

The whole IR region is usually divided into three ranges: near IR (NIR: from 800 nm to 2500 nm), mid IR (MIR: from 2.5 μm to 2500 μm) and far IR (FIR: from 2500 μm to 1 mm). Fundamental vibrations of the main combustive gas molecules are located in the MIR region, while in the NIR region overtones are mainly located, the absorption intensity being by several orders lower than for fundamental vibrations. That is why the MIR region is mainly used for NDIR measurements. However, the NIR LEDs optical power is higher by several orders than for the MIR ones, making the NIR a promising region for using the LEDs.

Most gases have absorption lines in the near IR range, i.e. between 1.3 and 2.3 μm . Fig. 1 shows the absorption coefficients for exhaust gases (upper panel) and the spectra of LEDs for exhaust gas analysis, as derived from the HITRAN database [14]. The typical content of an exhaust gas [15] is: 71% N_2 +14% CO_2 +13% H_2O +1.5% CO +0.5% CH_4 . Nitride oxides (NO and NO_2) concentrations are less than 0.5%. It makes NDIR sensors not the right solution for detecting nitride oxides. Typical characteristics for available multicomponent NDIR exhaust gas MIR sensors are given in Table I.

In our specific case we are using the prototype for multicomponent gas detection shown in Fig. 2 (a). As a source of radiation, we use a 6-element multi-wavelength LED matrix based on the heterostructure $GaInAsSb/AlGaAsSb$, with peak wavelengths at 1.3, 1.4, 1.6, 1.8, 2.0 and 2.3 μm [16] (see Fig. 2 (b)). In the measurement unit we used the semiconductor photodiode Lms24PD-20-TEM [16]. The measured wavelengths are 1.4, 1.6, 1.8, 2.0 and 2.3 μm for the detection of H_2O , CO_2 , CO and CH_4 absorption lines, respectively. These lines are characterized by the same width as the filter width in Table I. The reference wavelength is 1.3 μm . Up to now all NIR measurements are not fulfilled, they have been performed only for one measuring LED [13, 17]. In this work we discuss

simulations for LED arrays. For bi-component mixtures the simulations have been performed in [18] and now we demonstrate, that the results are almost identical for a larger number of components.

TABLE I. WAVELENGTH RANGE AND SPECTRAL WIDTH OF COMMERCIAL NDIR EXHAUST GAS DETECTORS

Gas	Wavelength, μm	Filter width, nm
CO	4.64	180
CO_2	4.26	180
CO_2	4.43	60
CO_2	4.33	160
N_2O	4.53	85
$CO+CO_2$	4.48	620
NO	5.3	180
HC	3.35-3.4	190
HC	3.46	163
HC	3.28-3.31	160
HC	3.09	160
HC	3.3-3.34	160
HC	3.42-3.451	160
HC	3.375-3.4	190
Reference channel	3.95	90

B. Multiwavelength analysis method

The proposed method is based on the integrated intensity measurement of radiation absorption of five matrix LEDs. This approach helps to calculate the corresponding concentrations of gases H_2O , CO_2 , CO and CH_4 . Since the peak of CO and CH_4 is covered near the wavelength 2.3 μm , an extra LED is tuned for CH_4 close to 1.6 μm . It helps to separate CO and CH_4 . Besides, the LED lines at 1.8 and 2.0 μm cover absorption lines of CO_2 and H_2O . That is why for their separation it is necessary to conduct an extra measurement on water absorption at 1.4 μm .

For absorption spectrum processing in a multicomponent gas environment, the mean least square analysis (MLS) is widely applied to the NDIR data. It is based on the minimization of mean least squares for a linear function of several parameters. Let us consider it for the case of multi component gas absorption. For rather small concentrations and optical paths, the Beer-Lambert law can be linearized. For gas transmittance, the following Beer-Lambert formula is given:

$$I = I_0 - \sum_k I_{0k} \alpha_k L \quad (1)$$

where α_k is the frequency dependent absorption coefficient, L – the optical path, I_{0k} – the Fourier components of the incident light, k – the wave vector and the sum goes over all wave vectors for specified LED spectra.

If noise is neglected, we could apply the least mean squares method (LMS) to linear relation (1) to directly extract the gas concentration from the experimental absorbance values.

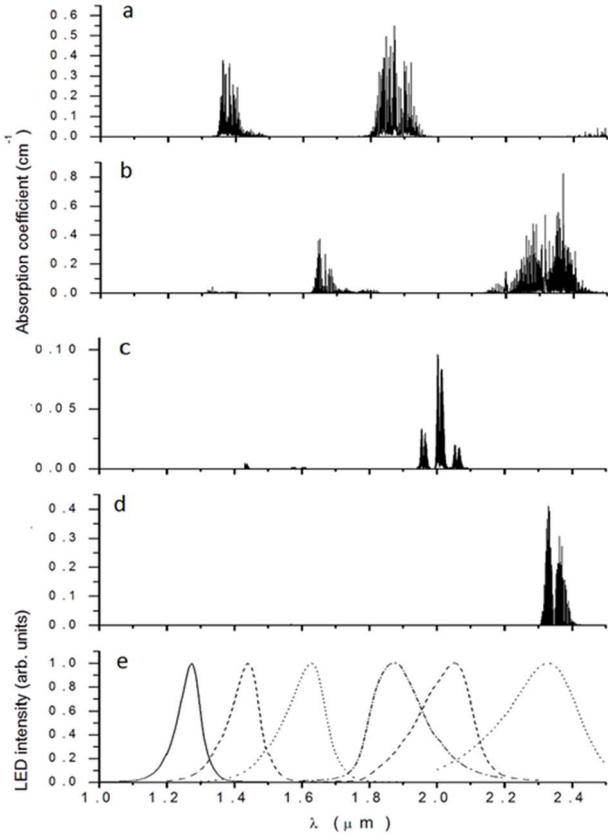
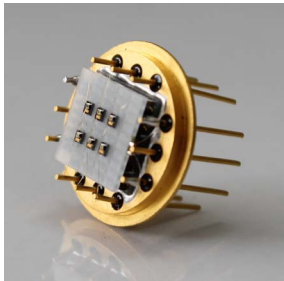


Fig. 1. Absorption coefficients of exhaust gases from HITRAN database [14] (a - H_2O , b - CH_4 , c - CO_2 , d - CO) and LED array spectra (e) in arb. units [16].



a



b

Fig.2. Photo of multicomponent gas detection prototype: a) –whole system, b) - 6-elements multi-wavelength LED chip

Using c_i for the concentration of the i -th gas component ($i=1$ to 4), φ_{ij} for the integral, over all LED spectra in Fig. 1, of the product of the i -th component absorbance by j -th LED intensity, we should minimize the sum:

$$\sum_j w_j (\sum_i c_i \varphi_{ij} - a_j)^2 \quad (2)$$

where a_j is the experimental absorbance for the j -th LED ($j=1$ to 5), w_j is the weight for the j -th LED line. To minimize the sum obtained in (2), the partial derivatives with respect to all concentrations c_i should be equal to zero, resulting in a set of linear equations:

$$\sum_{j,k} w_j \varphi_{ij} \varphi_{kj} c_k = \sum_j w_j \varphi_{ij} a_j \quad (3)$$

From the system of linear equations (3), the concentrations of all gas components could be derived, provided that the system is not degenerate, which is generally the case if spectra do not overlap strongly. Also the number of used LEDs should be not less than the number of gases in the mixture. In matrix form, the solution in (3) could be written as:

$$C = F^{-1} A \quad (4)$$

If absorbance values A are modeled by the Beer-Lambert formula, (4) restores all gas concentrations with very high accuracy.

III. SIMULATIONS

A. Noise effects

The only problem left is to correctly account for the noise, present in all experimental data. For uncorrelated noise in intensity we should use the same intensity in the left and in the right part of (3). At the same time we are not aware of the level of noise associated with the intensity measurement. For this reason, we substitute intensities in the left part in (3) with previously measured calibration LED spectra. Though the noise is statistically the same for the two cases, it is not identical, so that we should check whether such noise effects could affect the concentrations obtained by the LMS method. In addition, we simulate transmission spectra for the comparison with the experiment, not absorbance ones, hence we should also consider the effects of background noise.

The existence of the first I_0 term in (1) calls for the need of additional considerations on noise. Rewritten (4) is given:

$$C = F^{-1}(A + N) \quad (5)$$

where N denotes all kinds of background noise, so that the restored C -values will be the sum of real concentrations plus noise equivalent concentrations (NEC) characterizing the sensitivity of the concentration measurements. For one component such definition is rather trivial, but for a multicomponent system it is not so evident. Analysis of the

sensitivity to background noise for a multicomponent gas is given below.

For a photodiode, the lower limit of light detection is given by the intensity of incident light required to generate a current equal to the noise current. This limit is referred to as the Noise Equivalent Power (NEP). For our case, the photodiode NEP is $2.5 \cdot 10^{-12} \text{ W} / \text{ Hz}^{1/2}$. Using a LED with 100 nm^{-1} bandwidth and 1 mW output power, a relative intensity noise amounting to 0.14% of the emitted radiation power is obtained. This result is confirmed experimentally by direct measurement, as shown in Fig. 3. It means that the whole absorption effects should be more than 0.2% in order to be detected, which results in the restrictions on gas sensitivity. Absorption coefficients are given in Fig. 1 for 100% gas concentrations (HITRAN database). For one component gas the NEC value could be evaluated as $\sigma L_{abs}/L$, where σ denotes relative mean square noise, L_{abs} is the corresponding absorption length and L is the optical path. The absorption lengths for the used LED wavelength and gases are presented in Table II. It shows that absorption depth varies greatly: it is 30 cm for CH_4 and is up to 420 cm for CO_2 .

Noise affects the detection of low gas concentrations or concentrations at short optical path, e.g. around 10 cm. In this case the experimentally measured noise shown in Fig. 3 is equal to the absorption in gas environment. Table III presents NEC values for single-components of gases considered above for optical path 10 cm and theoretical noise value 0.14%.

TABLE II. ABSORPTION LENGTH (CM) AT 100 % CONCENTRATION

Gas\LED line	1.4	1.6	1.8	2.0	2.3
CO	$3.3 \cdot 10^6$	75812	$2 \cdot 10^8$	$9 \cdot 10^7$	288
CO ₂	14144	23698	1091	423	4071
H ₂ O	66	823	29	92	3213
CH ₄	1165	372	1451	1865	28

TABLE III. NOISE EQUIVALENT CONCENTRATION (NEC) FOR SEVERAL GASES (OPTICAL PATH 10 CM AND NEP VALUE $2.5 \cdot 10^{-12} \text{ W} / \text{ Hz}^{1/2}$)

	CO	CO ₂	H ₂ O	CH ₄
NEC %	4	6	0.4	0.4

The total measured noise is the sum of the noise in the LED intensity, and the noise associated with the preamplifier and the photodiode. Noise in the LED is characterized by the so-called relative intensity noise (RIN) parameter, which is the Fourier transform of the time average of the intensity autocorrelation function. The predominant source for the RIN is spontaneous emission. The total noise of a photodetector is basically the sum of its shot noise, Johnson-Nyquist thermal noise and dark current noise. The spectral density of thermal and shot noise is flat across a wide frequency range and it is usually modeled as white noise. The LED preamplifier and the driver also produce essentially white noise.

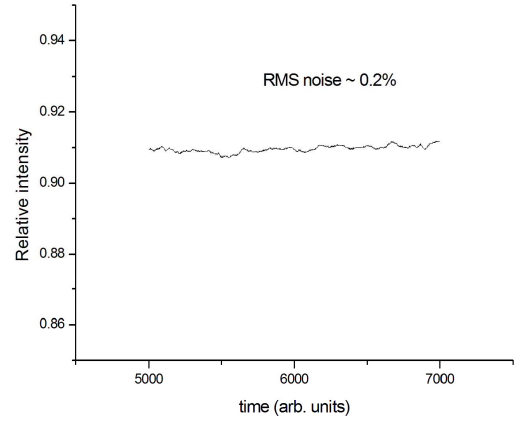


Fig. 3. Experimental root mean square noise of the LED with 2.3 μm wavelength.

B. Simulations of RIN and background white noise

In this section, we investigate how the effects of RIN and background white noise affect results obtained by the LMS method. All absorbance data simulations are done for the optical path of 10 cm and for the same gas mixture: 14% CO_2 +13% H_2O +1.5% CO +0.5% CH_4 . For the sake of simplicity we assume that the noise for all LED lines is the same.

To evaluate RIN effects, white noise is artificially added to the LED intensity (Fig. 4) and then it is used in the LMS calculations. We should note that using the same distribution in the right and left parts in (3), we model experimental spectra with a single noise distribution, while experimental calibration LED spectra have varying random noise. So different random noise distributions with the same root mean square noise were used for simulation of experimental data and LED calibration spectra. If the same random noises were added, the LMS method would reproduce the concentrations with very high accuracy. Results for the retrieved concentrations are given in Table IV (as could be seen, the numerical calculation errors are on the level of the 5-th digit). Table IV shows, that the RIN noise which is much stronger than the experimental one, results in small concentration errors, indicating the reliability of the method.

TABLE IV. MLS CONCENTRATIONS FOR DIFFERENT RIN NOISE

Normal RIN noise	CO %	CO ₂ %	H ₂ O %	CH ₄ %
0 %	1.501	14	13	0.5
0.5 %	1.54	14.01	13	0.496
1 %	1.58	14.02	13	0.491
1.5 %	1.63	14.03	13	0.487

To check the effects of background noise, one can add pure white noise to the right side in (5) and determine the concentrations of a multicomponent gas in this case. This

procedure could be used for the evaluation of the multicomponent sensitivity. Adding white noise with normal distribution, zero mean value and different values, one can solve (5) for gas concentrations. Results are presented in Table V.

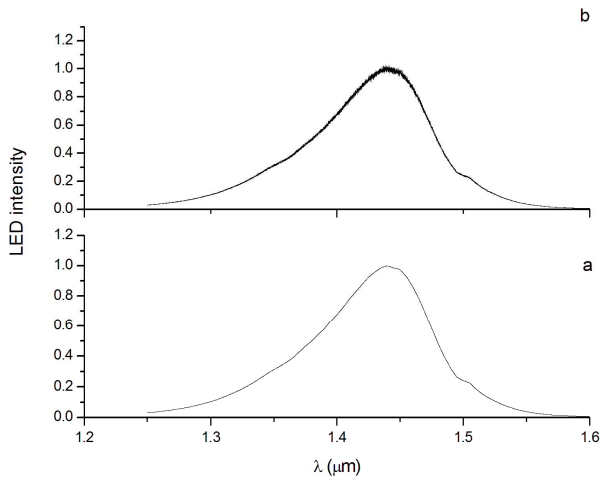


Fig. 4. LED spectra for noise effect simulations (a – initial, b – noise with normal distribution and with $\sigma=1\%$)

TABLE V. MLS CONCENTRATIONS FOR DIFFERENT BACKGROUND NOISE

%	CO %	CO ₂ %	H ₂ O %	CH ₄ %
0.014	1.07	13.986	13	0.504
0.021	0.856	13.979	12.999	0.563
0.028	0.641	13.972	12.999	0.584
0.035	0.426	13.965	12.999	0.605
0.042	0.211	13.958	12.998	0.626

Table V shows that the noise effect is much stronger than in the case of RIN noise. Furthermore, it shows that white noise mainly affects the CO concentration. The error in the derived concentration is of the same order as the error shown in Table III. Errors in Table V and Table III are in fact 0.4% and 4%, respectively, but the noise intensity is 10 times higher for the data in Table III. It is likely that CO is less sensitive and more affected by the noise as compared to other gases, because its IR absorption peak overlaps the methane one. In contrast, the CO₂ IR absorption peak, which is less intense than the CO one, does not suffer from the interference with other peaks. Hence it exhibits higher sensitivity and is less affected by the noise as compared to CO. To improve the situation with respect to CO detection, we need a larger optical path (as in the case of open path detectors).

IV. CONCLUSIONS

In this paper, we have presented an NDIR multicomponent gas analysis method based on IR multi-wavelengths in the range of 1.3 – 2.3 μm. As a source of radiation, we used a 6-element multi-wavelength LED matrix based on the

heterostructure GaInAsSb/AlGaAsSb with peak wavelengths at 1.3, 1.4, 1.6, 1.8, 2.0 and 2.3 μm. We applied this method to the analysis of gases concentrations of H₂O, CO₂, CO and CH₄ which are main components in the exhaust gas of a typical gasoline vehicle.

The proposed approach ensures the processing of measured data even in the case when the gas absorption lines are located close to each other and are covered by one radiation line of LED. Also, it does not require a complex multisensory platform which includes various analog and digital gas sensors [19, 20].

We have demonstrated that sensitivity of proposed solution is defined by background noise and depends on the LED radiation absorption which is affected by the length of optical path.

The results obtained in this work can be applied to the open-path detectors where a radiation source and receiver are located at the distance of tens of meters from each other. In particular, the application of the proposed method in tunnels and along the roads is a promising solution for air quality monitoring in the cities.

REFERENCES

- [1] M. Naphade, G. Banavar, C. Harrison, J. Paraszczak, R. Morris, "Smarter cities and their innovation challenges," IEEE Computer, vol. 44, no. 6, pp. 32-39, June 2011.
- [2] P. Penttinen, K. L. Timonen, P. Tiittanen, A. Mirme, J. Ruuskanen, J. Pekkanen, "Number concentration and size of particles in urban air: effects on spirometric lung function in adult asthmatic subjects," Environmental Health Perspectives, vol. 109, no. 4, pp. 319-323, 2001.
- [3] J. J. Li, B. Faltings, O. Saukh, D. Hasenfratz, J. Beutel, "Sensing the air we breathe - the OpenSense dataset," Proceedings of the 26th International Conference on Artificial Intelligence (AAAI), pp. 323-325, July 22-26, 2012, Toronto, Canada.
- [4] M. Ceriotti et al., "Is there light at the ends of the tunnel? Wireless sensor networks for adaptive lighting in road tunnels," Proceedings of the 10th International Conference on the Information Processing in Sensor Networks (IPSN), pp. 187-198, April 12-14, 2011, Chicago, IL, USA.
- [5] D. Hasenfratz, O. Saukh, C. Walser, C. Hueglin, M. Fierz, T. Arn, J. Beutel, L. Thiele, "Deriving high-resolution urban air pollution maps using mobile sensor nodes," Pervasive and Mobile Computing, vol. 16, part B, pp. 268-285, January 2015.
- [6] A. Somov, E. F. Karpov, E. Karpova, A. Suchkov, S. Mironov, A. Karelin, A. Baranov, D. Spirjakin, "Compact low power wireless gas sensor node with thermo compensation for ubiquitous deployment, IEEE Transactions on Industrial Informatics, vol. 11, no. 6, pp. 1660-1670, 2015.
- [7] G. L. Re, D. Peri, S. D. Vassallo, "Urban air quality monitoring using vehicular sensor networks," Advances in Intelligent Systems and Computing, Springer, vol. 260, pp. 311-323, 2014.
- [8] P. Vlacheas, R. Giaffreda, V. Stavroulaki, D. Kelaidonis, A. Somov, V. Foteinos, G. Poulios, A. R. Biswas, K. Moessner, P. Demestichas, "Enabling smart cities through a cognitive management framework for the internet of things," IEEE Communications Magazine, vol. 51, no. 6, pp. 102-111, 2013.
- [9] E. Medvedeva, A. Baranov, A. Somov, Design and investigation of thin film nanocomposite electrodes for electrochemical sensors, Sensors and Actuators, B: Chemical, 2016
- [10] L. P. Oleksenko, N. P. Maksymovych, E. V. Sokovykh, I. P. Matushko, A. I. Buvailo, N. Dollahon, "Study of influence of palladium additives in nanosized tin dioxide on sensitivity of adsorption semiconductor sensors to hydrogen," Sensors and Actuators B: Chemical, vol. 196, pp. 298-305, June 2014.

- [11] A. Makeenkov, I. Lapitskiy, A. Somov, A. Baranov, "Flammable gases and vapors of flammable liquids: Monitoring with infrared sensor node," *Sensors and Actuators, B: Chemical*, vol. 209, pp. 1102-1107, 2015.
- [12] J. Hodgkinson and R. Tatam, "Optical gas sensing: a review," *Meas. Sci. Technol.* **24**, 012004, 2013.
- [13] S. Fanchenko, A. Baranov, A. Savkin, A. Petukhov, K. Kalinina, B. Zhurtanov, M. Velikotny. "Non-dispersive LED-based methane open path detector capabilities," *Proceedings IEEE Workshop on Environmental, Energy, and Structural Monitoring Systems, 2015, EESMS 2015*, pp. 146-151, Trento, Italy 9-10 July 2015.
- [14] L.S. Rothman, R.R. Gamache, A. Goldman, L.R. Brown, R.A. Toth, H.M. Pickett, R.L. Poynter, J.-M. Flaud, C. Camy-Peyret, A. Barbe, N. Husson, C.P. Rinsland, and M.A.H. Smith, "The HITRAN database: 1986 Edition," *Appl. Opt.* **26**, 4058-4097 (1987).
- [15] http://www.volkspage.net/technik/spp/spp/SSP_230.pdf (January 2016).
- [16] LED Microsensor NT (<http://ru.lmsnt.com>, January 2016).
- [17] S. Fanchenko, A. Baranov, A. Savkin, V. Sleptsov, "LED-based NDIR natural gas analyzer," *IOP Conference Series: Materials Science and Engineering* **108**, 012036, 2016.
- [18] S. Fanchenko, A. Baranov, A. Savkin, A. Petukhov, K. Kalinina, B. Zhurtanov, M. Velikotny. "Multicomponent hydrocarbons monitoring by infrared LED arrays," *Proceedings IEEE Workshop on Environmental, Energy, and Structural Monitoring Systems, 2016, EESMS 2016*, pp. 122-125, Bari, Italy 13-14 June 2016.
- [19] Denis Spirjakin, Alexander Baranov, Alexey Karelin, Andrey Somov, "Wireless multi-sensor gas platform for environmental monitoring," *Proceedings IEEE Workshop on Environmental, Energy, and Structural Monitoring Systems, 2015, EESMS 2015*, pp. 232-237, Trento, Italy 9-10 July 2015.
- [20] D. Hasenfratz, O. Saukh, S. Sturzenegger, L. Thiele, "Participatory air pollution monitoring using smartphones," *Proceedings of the 2nd International Workshop on Mobile Sensing*, pp. 1-5, April 16-20, 2012, Beijing, China.